

1 **Urban scale air quality modelling using detailed traffic emissions estimates**

2

3 C. Borrego¹, J.H. Amorim^{1,2*}, O. Tchepele^{1,3}, D. Dias^{1,3}, S. Rafael¹, E. Sá¹, C. Pimentel¹, T. Fontes^{4,5}, P.
4 Fernandes⁴, S.R. Pereira⁴, J.M. Bandeira⁴, M.C. Coelho⁴

5 ¹University of Aveiro, Centre for Environmental and Marine Studies (CESAM), Department of
6 Environment and Planning, Campus Universitário de Santiago, 3810-193 Aveiro, Portugal

7 ²Swedish Meteorological and Hydrological Institute (SMHI), Air quality research unit, SE-60176
8 Norrköping, Sweden (present address)

9 ³CITTA, Department of Civil Engineering, University of Coimbra, Polo II, 3030-788 Coimbra, Portugal
10 (present address)

11 ⁴University of Aveiro, Centre for Mechanical Technology and Automation (TEMA), Department of
12 Mechanical Engineering, Campus Universitário de Santiago, 3810-193 Aveiro, Portugal

13 ⁵Faculty of Engineering, Department of Industrial Management, University of Porto, Rua Roberto Frias,
14 4200-465, Porto, Portugal (present address)

15 *Corresponding author: jorge.amorim@smhi.se

16

17 **Abstract**

18 The atmospheric dispersion of NO_x and PM₁₀ was simulated with a second generation Gaussian model
19 over a medium-size south-European city. Microscopic traffic models calibrated with GPS data were used
20 to derive typical driving cycles for each road link, while instantaneous emissions were estimated
21 applying a combined Vehicle Specific Power/Co-operative Programme for Monitoring and Evaluation of
22 the Long-range Transmission of Air Pollutants in Europe (VSP/EMEP) methodology. Site-specific
23 background concentrations were estimated using time series analysis and a low-pass filter applied to
24 local observations. Air quality modelling results are compared against measurements at two locations
25 for a 1 week period. 78% of the results are within a factor of two of the observations for 1-h average
26 concentrations, increasing to 94% for daily averages. Correlation significantly improves when
27 background is added, with an average of 0.89 for the 24 hours record. The results highlight the potential
28 of detailed traffic and instantaneous exhaust emissions estimates, together with filtered urban
29 background, to provide accurate input data to Gaussian models applied at the urban scale.

30

31 **Keywords**

32 Urban air quality; Gaussian model; traffic modelling; emissions modelling; monitoring campaign;
33 background concentration

34

35 **1. Introduction**

36 In the European Union 72% of the population lives in urban areas, a rate that is projected to increase
37 (EEA, 2015a). Despite significant efforts to improve urban air quality, namely by reducing traffic

38 emissions (Tente et al., 2011; Cyrysa et al., 2014), air pollution is still the single largest environmental
39 health risk in Europe (EEA, 2015b). Over the past years, and due to policy pressures requiring more
40 detailed assessment of air pollution at local and urban scales, there has been a growing need to simulate
41 meteorological and air quality fields at higher spatial resolutions than the ones obtained with mesoscale
42 models (Coelho et al., 2014). Regardless the increasing application of high-resolution computational
43 fluid dynamics (CFD) models over cities (Amorim et al., 2013a; Martins et al., 2009), the large demand of
44 input data and the computationally expensive simulations still represent an obstacle when dealing with
45 large areas and/or long-term periods. Hence, Gaussian models constitute a natural choice for the urban
46 scale air pollutant dispersion modelling with regulatory or policy assessment purposes (Zawar-Reza et
47 al., 2005; Gidhagen et al., 2009), especially in the simulation of short-range (up to a few tenths of
48 kilometers from the emission source) dispersion processes from different sources over topographies of
49 varying complexity, inclusively accounting for building-induced effects (Denby, 2011). Also, background
50 concentrations are of particular interest, because they are a critical source of uncertainty in the
51 prediction of ambient levels (Stein et al., 2007; Arunachalam et al., 2014). Reliable estimates of
52 background concentrations are indispensable for accurate air dispersion modelling results. However,
53 there are several techniques that may be used for this purpose and their selection may influence the
54 final results.

55 Despite the developments on air quality models, road traffic emissions are still a variable of
56 fundamental relevance in the global accuracy of simulations, especially at the urban scale. Whereas
57 instantaneous emission models (such as CMEM and VT-micro) are based on second-by-second vehicle
58 dynamics and clearly include congestion in the modelling process, the emission rates used by average
59 speed models (such as COPERT) are calculated based on standardized driving cycles (Smit et al., 2008).
60 Although Ahn and Rakha (2008) pointed out that the use of instantaneous emission models is the most
61 appropriate method to assess different operational traffic scenarios, the majority of the studies linking
62 road traffic, emission, air quality and human exposure at the urban scale usually use average speed
63 emission models (Mensink and Cosemans, 2008; Amorim et al., 2013b). As exceptions one can mention
64 the studies conducted by Amirjamshidi et al. (2013) and Misra et al. (2013), in which PARAMICS traffic
65 model was linked to CMEM emission model and an air quality model to estimate the levels of carbon
66 monoxide (CO), nitrogen oxides (NO_x) and hydrocarbons (HC).

67 Given this background, the present paper proposes the simulation of air quality at the urban scale based
68 on a detailed traffic modelling approach that uses microscopic traffic models calibrated with real world
69 GPS data in order to establish typical driving cycles for each link within the road network. The
70 atmospheric dispersion of NO_x and particulate matter (PM), both pollutants posing serious health
71 concerns in urban areas, is calculated with a second generation Gaussian model, accounting for the
72 effect of buildings. Background contribution to urban air pollution levels is estimated with a low-pass
73 filter applied to local observations. Modelling results are compared against field observations in a south-
74 European city.

75

76 **2. Methodology**

77 The Portuguese city of Aveiro was selected as study area because of the adequate size and relevant road
78 network for the purpose of the work, the prior availability of traffic volume data (both from Aveiro
79 municipality as from previous measurements performed by the authors), as also the facilitated logistics
80 in the set-up of experimental campaigns. This medium-size city, with approximately 198 km² and 78
81 thousand inhabitants (INE, 2013), is located at the Norwest coastline at 70 km south of Porto. The
82 following sections describe the experimental observations (section 2.1) and the numerical modelling
83 approach (sections 2.2 to 2.4).

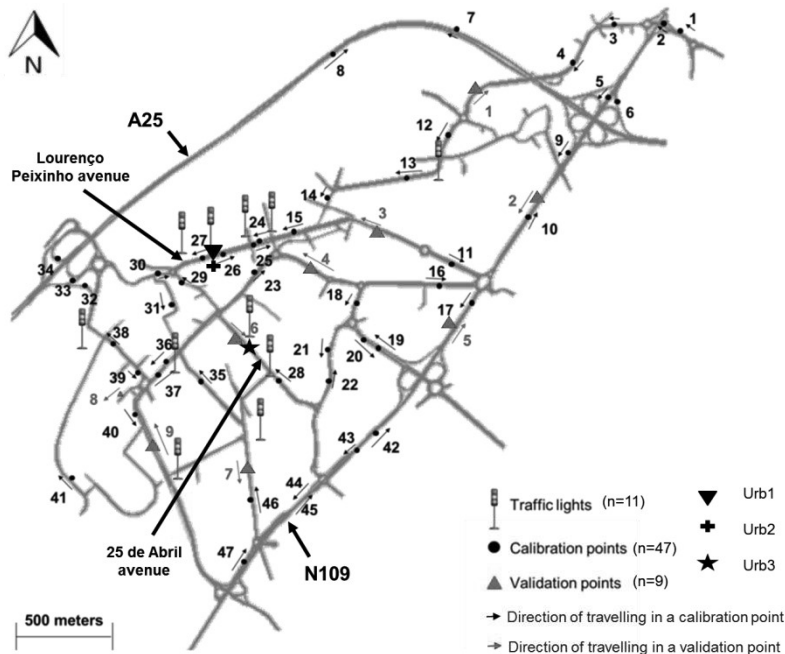
84

85 2.1. Experimental field campaigns

86 The experimental work consisted in the monitoring of road traffic, meteorological conditions, and air
87 pollutant concentrations for selected periods in different locations within the city, as hereafter
88 described. Emissions were not directly measured during the field campaigns.

89 To assess the road traffic network several variables were collected. Firstly, ten different routes with
90 heterogeneous traffic conditions across the study domain were covered using GPS data-logger equipped
91 vehicles to collect second-by-second vehicle dynamics (speed, acceleration/deceleration and road
92 grade). GPS data includes road traffic field campaigns performed during peak (7-10h and 17-19h) and
93 non-peak (10-17h) periods on typical weekdays (Tuesdays to Thursdays) and under dry weather
94 conditions in February/March 2011, February/March 2012 and May/June 2013. Approximately 550 km
95 of GPS data over 15 hours were considered during peak hours, allowing the coverage of congested
96 periods. For validation purposes, the authors used 15 data sets of vehicle dynamic data from 10
97 different routes. Such monitoring routes included urban roads, arterials, and motorways over the study
98 domain (with different traffic flows and speed limits). In addition, aiming to reduce systematic errors,
99 road tests were performed using different drivers and vehicles.

100 Traffic was monitored in 56 strategic points that allow the connection among the most important roads
101 within the study network, as shown in Figure 1. Based on the above data, time dependent origin-
102 destination (O/D) matrices were defined for each intersection and assigned to the overall study domain.
103 To monitor traffic signals timing, the cycle length and phasing was measured six times in the traffic lights
104 in five points of the domain. A detailed description of the field work for vehicle dynamics assessment
105 and traffic monitoring can be found in *Bandeira et al. (in press)* and *Fontes et al. (2014)*.



106

107 **Figure 1.** Study domain showing the traffic collection points and the location of the urban air quality stations (the
108 suburban background station is outside the domain). Main roads are indicated: A25 (motorway), 'Lourenço
109 Peixinho' (city avenue), '25 de Abril' (city avenue), and N109 (interurban road).

110

111 Aiming to capture the spatial variation of air quality a monitoring network consisting of four stations
was designed, as shown in Figure 1 and Table 1. The air pollutants addressed in this paper are NO_x and

112 particles with an aerodynamic diameter smaller than 10 μm (PM₁₀). Air quality monitoring equipment
 113 with similar technical specifications was used in the different stations. Two of them were located in
 114 major thoroughfares of the city, the ‘Lourenço Peixinho’ avenue (labelled as Urb1 and shown in Figure
 115 2a) and the ‘25 de Abril’ avenue (Urb3). The Urb2 station (Figure 2b) was positioned in a pedestrian zone
 116 with very low traffic density. Although it was located at close distance from the avenue, the buildings
 117 geometry protects this location from the direct influence of traffic emissions. Finally, data from a
 118 suburban background station (Sub), located at approximately 6.5 km from Urb1, are included in the
 119 analysis.



120 **Figure 2.** Mobile air quality monitoring stations (a) Urb1 (b) and Urb2.

121 **Table 1.** General description of the air quality stations.

Station ID	Classification	Type	Location
Urb1	Urban (traffic)	Mobile	Central sidewalk of the ‘Lourenço Peixinho’ Av. 40°38’31’’ N; 8°39’03’’ W
Urb2 ⁽¹⁾	Urban (traffic)	Mobile	Square in front of the ‘Manuel Firmino’ market (ca. 100 m from Urb1) 40°38’30’’ N; 8°38’58’’ W
Urb3 ⁽²⁾	Urban (traffic)	Fixed	Front yard of the ‘José Estêvão’ School, in the ‘25 Abril’ Av. (ca. 570 m from Urb1) 40°38’08’’ N; 8°38’48’’ W
Sub ⁽²⁾	Suburban (background)	Fixed	‘Gabriel de Ançã’ School, in Ílhavo town (ca. 6.5 km from Urb1) 40°35’23’’ N; 8°40’14’’ W

122 ⁽¹⁾Used to characterize background concentration (cf. sections 2.4 and 3.1)

123 ⁽²⁾Station from the national network QUALAR (<http://www.qualar.org>),
 124 managed by the Portuguese environmental agency APA.

125

126 In addition, wind velocity, wind direction, temperature, and relative humidity were measured using 10
 127 m high meteorological masts installed in the mobile labs. A 1 week study period was defined between
 128 the 1st (9h) and the 8th (14h) of June 2013, in a total of 174 hours. In the case of Urb1 observations of
 129 PM₁₀, the time period covered by this analysis is shorter (91 hours) in order to fulfill with the minimum
 130 data acquisition efficiency of 75%.

131

132 2.2. Road traffic modelling

133 The simulation of road traffic at the urban scale was carried out applying the VISSIM (‘Verkehr In Städten
 134 SIMulationsmodell’) microscopic traffic model (PTV, 2011) tuned with the traffic data field
 135 measurements. This model was selected because of the possibility of defining different road-user

136 behavior parameters and selecting sub-models (car following, lane change and gap acceptance) for
137 distinct vehicle types. Additionally, it allows the definition of vehicles performance outputs, such as
138 desired maximum speed per vehicle and class (PTV, 2011). Several studies have documented the
139 effective use of this tool in assessing management strategies in real world case studies (Mahmod et al.,
140 2010; Fontes et al., 2014; Fernandes et al., 2016).

141 VISSIM was used to simulate individual vehicle movements during peak and non-peak periods aiming to
142 consider the variability in traffic dynamics throughout a typical working day. Traffic model parameters
143 were calibrated by modifying vehicle performance and driver behavior parameters and examining their
144 effect on traffic flows and speeds in 47 points of the study domain, as depicted in Figure 1. The driver
145 behavior parameters included car-following (average standstill distance, additive and multiple part of
146 safety distance), lane-change and gap acceptance (front gap, rear gap, safety factor, anticipate route),
147 and simulation resolution. The methodology presented in Fontes et al. (2014) was followed.

148 Traffic model validation focused on comparing estimated and observed hourly traffic flows in the points
149 that were not used for calibration, as well as travel time, average speeds and cumulative VSP modes
150 distributions for each monitoring route. This procedure was conducted with a preliminary number of
151 simulation runs (between 10 and 20, as suggested by Hale, 1997). The widely-accepted FHWA (Federal
152 Highway Administration) practice Geoffrey E. Havers (GEH) statistic was used to compare estimated and
153 observed traffic flows. The advantage of using GEH is that it avoids divisions by zero and is independent
154 of the order of the values. Aiming to satisfy the validation criteria, the GEH should be less than 5 for at
155 least 85% of the monitoring points (Dowling et al., 2004).

156 For travel time and average speed, the root-mean-square percentage error (RMSPE) was used to
157 measure the magnitude of the errors between data samples. This goodness-of-fit measure was selected
158 for two main reasons: it provides comparing forecasting errors of different models for specific variables;
159 and the validation parameters values are significantly higher than zero which avoids extremely skewed
160 distributions (Hyndman and Koehler, 2006).

161 Lastly, the observed (GPS runs) and estimated (VISSIM output) VSP modes distributions were calculated
162 from travel time data of each monitoring route, and further compared using the two-sample
163 Kolmogorov-Smirnov test (K-S test) for a 95% confidence level. K-S evaluates the consistency between
164 the estimated and observed VSP mode distributions, and it is suggested when a natural ordering of the
165 modes of data samples occurs (Fontes et al., 2014).

166

167 2.3. Vehicles emission modelling

168 As mentioned, vehicular emissions were not measured at the site. Thus, emission estimates were
169 carried out by using two complementary methodologies: VSP (EPA, 2002; Frey et al., 2008; Coelho et al.,
170 2009) was used to estimate the emissions of NO_x and PM for passenger cars and light duty vehicles,
171 while for heavy duty vehicles and motorcycles, the EMEP/EEA methodology (EEA, 2013) was applied
172 since there is a lack of VSP emission factors adapted to the European situation. The VSP methodology
173 allows estimating second-by-second emissions based on vehicle's dynamics (speed, acceleration and
174 road grade) in accordance to the specified level of detail of the road traffic model used previously.
175 Because of its direct physical interpretation and strong statistical correlations with vehicle emissions,
176 VSP has become a widely recognized approach for emission micro simulation from both gasoline (EPA,
177 2002; Frey et al., 2008) and diesel (Zhai et al., 2011) light passenger vehicles. Total emissions by segment
178 can be derived based on the time spent in each VSP mode multiplied by its respective emission factor
179 (EPA, 2002; Frey et al., 2008). More information on the VSP methodology is described in Frey et al.
180 (2008), EPA (2002), and Coelho et al. (2009). In the EMEP/EEA methodology (EEA, 2013) the emission

181 factors depend on the speed, age and engine size or tonnage of each vehicle category. Although this
182 methodology is based on the average speed, in order to maintain consistency, the emission factors were
183 adapted to consider the spatiotemporal resolution of the other models.

184 Emissions estimates using VSP/EMEP methodologies were based on vehicle dynamics data
185 (instantaneous speed, acceleration/deceleration) gathered from VISSIM traffic model which had been
186 calibrated with GPS data. A console application in C# programming language was developed to compute
187 second-by-second vehicle dynamics data from VISSIM output. Passenger cars total emissions were
188 based on Portuguese fleet according to the information given by the Portuguese Automotive Association
189 (ACAP): 57.5% passenger gasoline vehicles and 42.5% of passenger diesel vehicles (ACAP, 2010).

190

191 2.4. Air quality modelling

192 Air pollution levels at the urban scale were simulated applying the air quality modelling system URBAIR
193 AIR (URBAIR) (Borrego et al., 2014; Valente et al., 2014). In its core is an improved version of the second
194 generation Gaussian model POLARIS (Borrego et al., 1997), which differs from traditional Gaussian
195 dispersion models because its dispersion parameters have a continuous variation with the atmospheric
196 stability and accounts for building-induced dispersion mechanisms. This steady state atmospheric
197 dispersion model is based on boundary layer scaling parameters and is suitable to be used for distances
198 up to about 10 km from the source. A pre-processor calculates the meteorological parameters needed
199 by the dispersion model, such as atmospheric turbulence characteristics, mixing height, friction
200 velocity, Monin-Obukov length and surface heat flux. The inputs consist of meteorological
201 measurements from a local synoptic surface station (located at the University of Aveiro, 1 km from
202 Urb1) and twice-daily upper air soundings (station 08001 over La Coruna, Spain, available at
203 <http://weather.uwyo.edu/upperair/sounding.html>). NO_x is treated as a non-reactive tracer, allowing
204 that the atmospheric chemistry involved is simplified to a steady state solution. Dry deposition fluxes of
205 particulate and gases are described applying conventional resistance schemes by Wesely et al. (2002).

206 The simulation domain defined over Aveiro, with dimensions of 3.9 x 4.5 km², coincides with the one
207 considered for the estimation of traffic dynamics and related emissions, covering the entire urban zone,
208 as shown in Figure 1. In order to use the emissions as estimated in section 2.3, URBAIR's road traffic
209 emissions module was deactivated. Line sources are discretized into a series of point sources with
210 diameters matching the road dimensions, following Karamchandani et al. (2009). No industrial sources
211 exist within the simulation domain, being the nearest one at approximately 5 km from the city center.
212 The contribution of industrial areas around the city is accounted in the urban background concentration,
213 as also for other point sources inside the domain (e.g., some bakeries using wood burning ovens).

214 Input data describing the spatial variation of terrain surface elevation, buildings 3D coordinates and
215 roads 2D coordinates are required. Local Geographic Information System (GIS) shapefiles complemented
216 with aerial imagery were used for this purpose. For simplicity, buildings were assembled based on
217 proximity and geometry criteria. Direction-specific downwash parameters, in the form of projected
218 building height and width dimensions, are estimated using an approach similar to the one implemented
219 in EPA's Building Profile Input Program for the Plume Rise Model Enhancements (BPIP-PRIME) model
220 (Schulman et al., 2000; EPA, 2004).

221 With the purpose of estimating representative background concentrations, several approaches have
222 been tested. In the scope of this work, the background concentration is defined as the concentration
223 that would be measured in the absence of local emission sources that are explicitly considered by the
224 dispersion model. Therefore, the background air quality should include a contribution of all other
225 sources, natural and anthropogenic, except local traffic emissions considered in the model inputs. As a
226 first attempt, measurements from the nearest suburban background station (Sub) carried out in June
227 2013 were analyzed, but this station poorly explains the fluctuations of the pollution levels within the
228 study area for the period of interest (cf. section 3.1). Therefore, an alternative approach previously
229 developed and validated by Tchepel and Borrego (2010) and Tchepel et al. (2010) was applied to define

230 the background pollution levels. The main idea of the data filtering is based on the assumption that the
231 fluctuations presented in the time series could be analyzed as a linear combination of periodic functions.
232 The contribution of local sources is attributed to high frequencies (short-term fluctuations). Therefore,
233 the filter is designed to remove the high frequencies and to pass the low frequencies presented in the
234 data. It should be noted that due to the filter algorithm, the length of the processed time series is
235 shorter than the original one but the data are still with hourly resolution.

236 The modelling results were evaluated against the measurements carried out in Urb1 and Urb3 stations
237 applying the model acceptance criteria proposed by Chang and Hanna (2004) for air quality models
238 assessment, which establishes performance measures for the normalized mean square error
239 (NMSE<1.5), fraction of predictions within a factor of two of observations (FAC2>0.5), and fractional bias
240 ($|FB|<0.3$). Also the correlation coefficient (r) was considered in the analysis. The performance
241 measures were calculated applying the BOOT Statistical Model Evaluation Software Package (Chang and
242 Hanna, 2004).

243

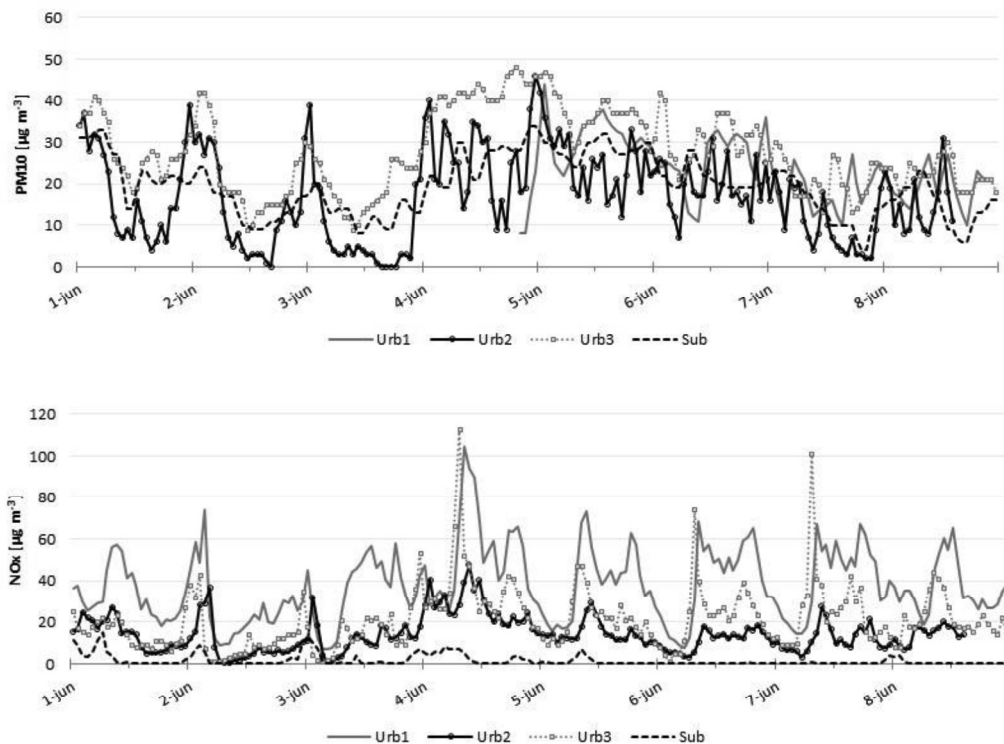
244 3. Results and discussion

245 In the following sections both monitored and modelled results are presented and analyzed.

246 3.1. Local measurements

247 Meteorological data on wind direction and velocity collected in Urb1 station from June 1 to 8 reveal a
248 dominant wind from North (24% of the time) and North-northwest (44%) with an average speed of 2
249 $m.s^{-1}$. South winds (18%) were registered mainly during the morning hours. The temperature ranged
250 between 12 and 28 °C and the relative humidity from 32 to 90%.

251 The observed pollutant concentration time series shown in Figure 3 reveals both daily and weekly
252 cycles, with a direct relation with the vehicle traffic and resulting emissions.



253 **Figure 3.** Hourly averaged concentration of PM₁₀ and NO_x measured in the four air quality stations from 1-8 June,
254 2013.

255 No exceedances to the limit values established by Directive 2008/50/CE (200 $\mu\text{g}\cdot\text{m}^{-3}$ hourly
256 concentration of nitrogen dioxide (NO_2) and 50 $\mu\text{g}\cdot\text{m}^{-3}$ daily concentration of PM10) were observed
257 during the reporting period. In comparison with the observations carried out in Urb1 station, lower
258 hourly mean concentrations and a smoother variation over time is found at Urb2 location as a
259 consequence of the longer distance to the main road. The statistical comparison between 1 month
260 (June) time-series acquired in Sub and Urb3 shows a low correlation ($r=0.21$) for daily average NO_x
261 values. Although for PM10 a better agreement ($r=0.65$) was obtained, the magnitude presented in the
262 suburban measurements is higher than that from the urban station. This indicates that Sub is not
263 representative of Aveiro's background in the period under analysis, which can potentially be associated
264 with emission sources in the vicinity of Sub, such as from the nearby city of Ílhavo or/and from
265 agricultural practices (given the predominantly rural characteristics of the site).

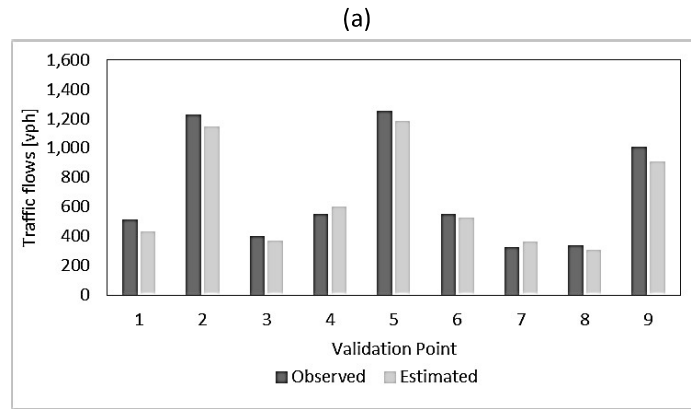
266

267 3.2. Road traffic

268 Figure 4 exhibits the validation results for the modeling platform of traffic and emissions and
269 corresponding statistic test with 10 different runs (stochastic traffic flow), as suggested by Hale (1997).
270 Figure 4a confirms that all traffic points recorded GEH values below 4, meeting the validation criteria
271 (Dowling et al., 2004). These findings are particularly significant since this study domain has a
272 considerable size with different traffic flows along main arterials (300 - 1,250 vph). The comparison
273 between observed and estimated travel time (Figure 4b) and speed (Figure 4c) resulted in a RMSPE
274 below 10% and within confidence level intervals. In such cases, the highest differences were found in
275 routes 7 and 8, which contained several uninterrupted traffic facilities (traffic lights, single or two-lane
276 roundabouts) throughout their length. Concurrently, each monitoring route showed a similar trend for a
277 97.5% confidence level ($p\text{-value} > 0.025$) concerning the comparison between observed and estimated
278 cumulative VSP modes distributions. Based on these validation results, 10 simulation runs were
279 considered to be appropriate to reproduce site traffic operations in VISSIM model, in agreement with
280 Dowling et al. (2004) and Hale (1997).

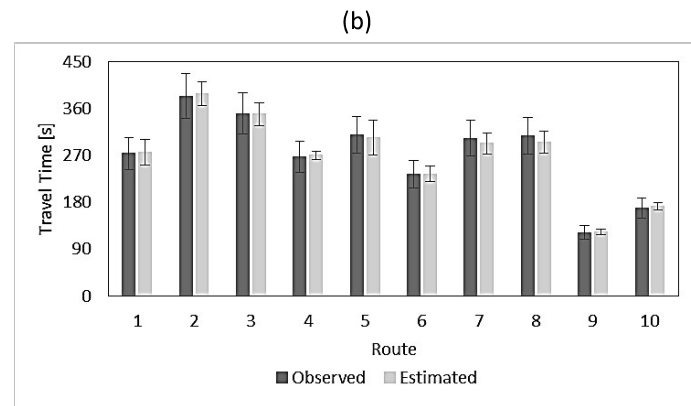
281

282



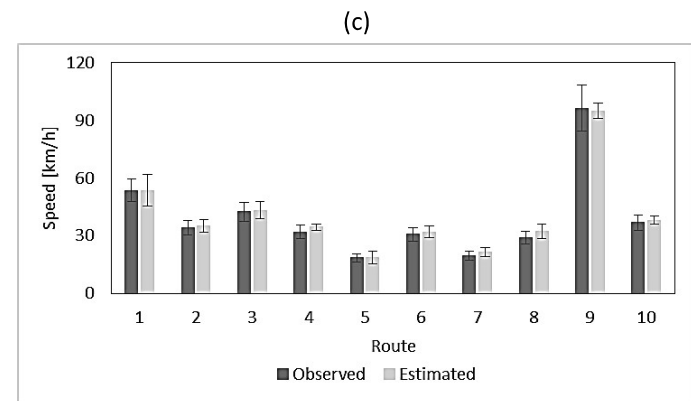
283

284



285

286



287

288

289

290

291

292

293

Figure 4. Validation results of traffic model: (a) traffic flow, (b) travel time, and (c) speed. Validation points were randomly selected in order to maintain consistency of the traffic flows and the remaining roads of the study domain.

293

3.3. Vehicles emission

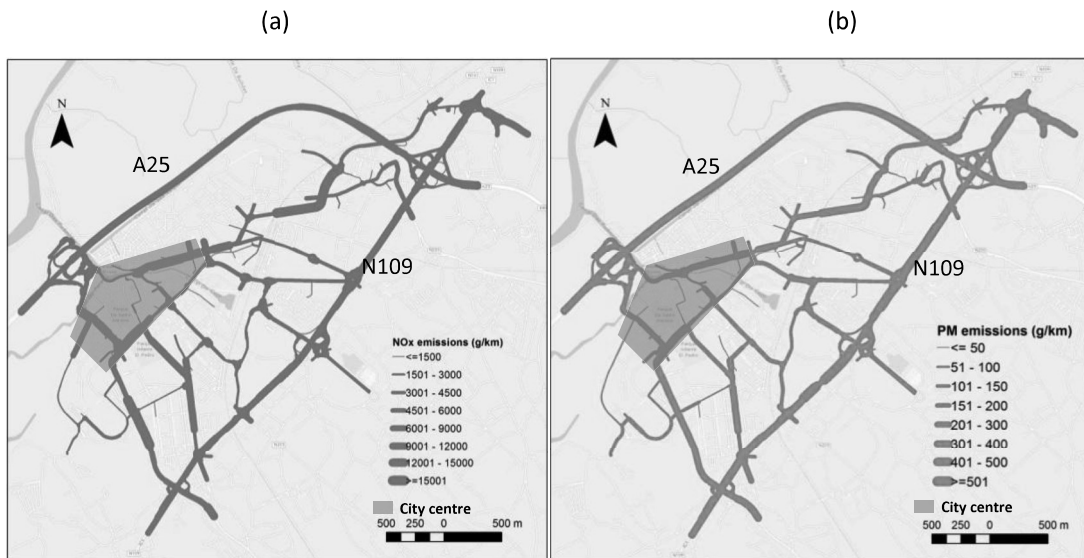
294

295

296

Figure 5 shows the daily emissions of NO_x and PM_{10} ($\text{g}\cdot\text{km}^{-1}$) recorded for the urban area of Aveiro. High emission hot-spots are achieved in the city center, where the daily average speed is low ($<50 \text{ km}\cdot\text{h}^{-1}$), as well as in the interurban road N109 and the motorway A25.

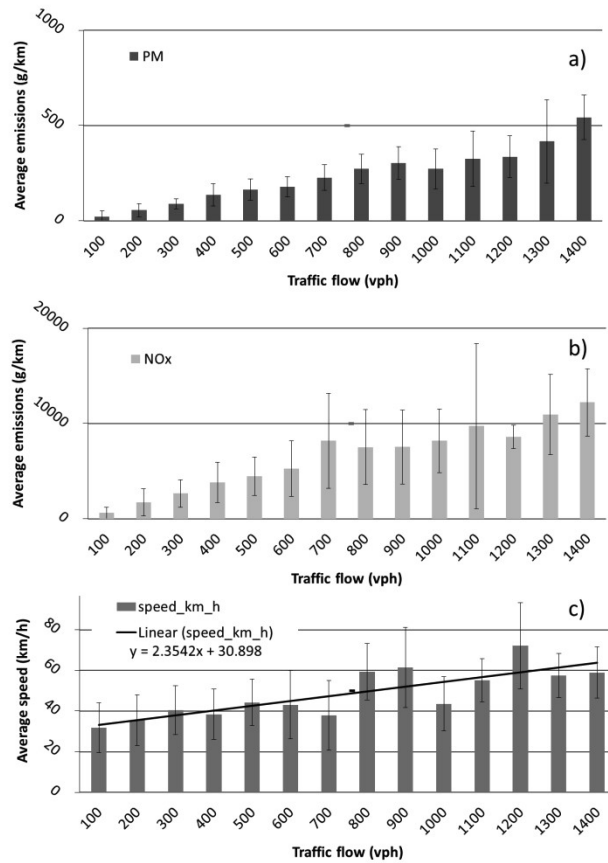
297



298

299 **Figure 5.** Daily emissions of (a) NO_x and (b) PM_{10} estimated for the city of Aveiro over a working day.

300 Figure 6 presents the average emissions by link for PM_{10} and NO_x ($\text{g}\cdot\text{km}^{-1}$) as a function of traffic flow
 301 (vph) and speed ($\text{km}\cdot\text{h}^{-1}$). The results show that more than 70% of total PM_{10} and NO_x emissions are
 302 generated in high-traffic demand areas (>800 vph), as depicted in Figure 6a and 6b. In these areas,
 303 speed is usually higher than $50 \text{ km}\cdot\text{h}^{-1}$ (Figure 6c). Two main reasons contribute for these results: firstly,
 304 roads with high traffic demand (e.g. N109 and A25) are characterized by high demand of heavy duty
 305 vehicles (especially when compared with city center roads); and secondly, traffic flow on the N109 and
 306 A25 roads can be severely impacted during peak hours affecting speed and travel time (see the high
 307 standard deviation of these links in Figure 6c), and as result increasing vehicular emissions occur. On the
 308 other hand, in the city center several intersections with traffic lights and roundabouts are presented
 309 (see Figure 1 for those details) which increases stop-and-go situations. Consequently, these speed
 310 changes contribute to increased total emission levels per vehicle.



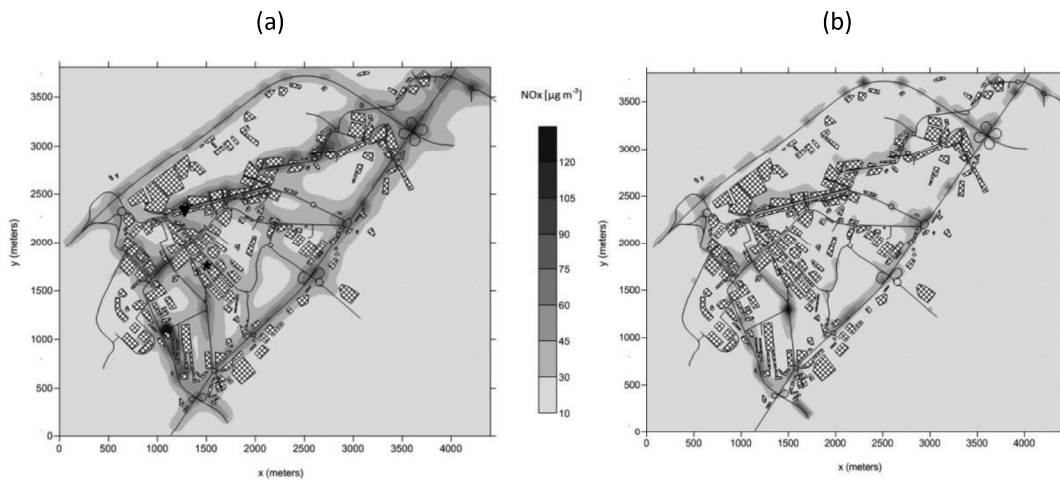
311

312 **Figure 6.** Estimates by link for the city of Aveiro: (a) average PM10 emissions; (b) average NOx emissions; and (c)
 313 average speed (c) as a function of average traffic flow.

314

315 3.4. Air quality

316 Figure 7 illustrates the response of URBAIR to peak vs off-peak conditions. The dynamics of traffic (and
 317 related emissions, as already discussed in Figure 5) and atmospheric conditions become evident in the
 318 magnitude and location of the NO_x hot-spots.

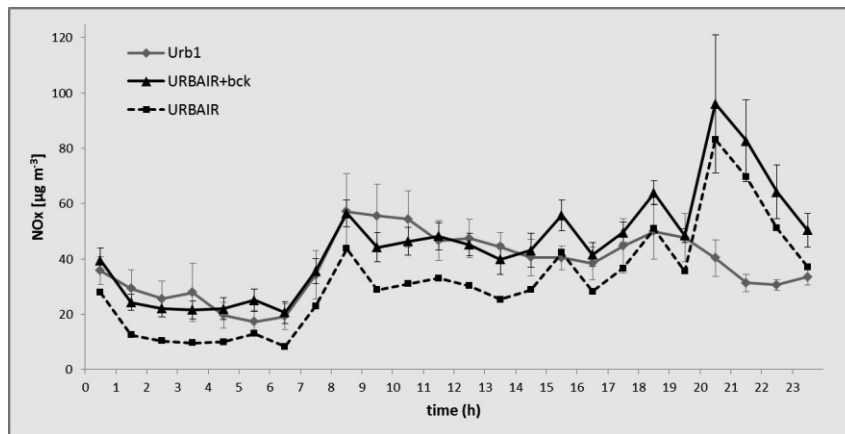


319

320 **Figure 7.** Contours of NO_x concentration fields simulated by URBAIR (with background levels added) over the city of
 321 Aveiro for (a) peak (8-9h) and (b) off-peak (13-14h) traffic conditions on the 6th of June 2013 (Thursday). Buildings

322 shown in crossed pattern. Symbols have the same meaning as in Figure 1. At Urb1 location, observ./model pairs are
323 the following: 68,1/69,4 $\mu\text{g.m}^{-3}$ (peak) and 44,0/39,3 $\mu\text{g.m}^{-3}$ (off-peak).

324 Aiming to further investigate the dependency of model performance on the time of the day, observed vs
325 computed daily mean profiles of hourly surface pollutant concentration were calculated. Figure 8
326 depicts the ability of the modelling approach to track the evolution of NO_x levels, including the morning
327 traffic peak at 8-9h. Similar agreement was observed for PM_{10} (not shown). However, an evident
328 overestimation is reported at the end of the day. This behavior originates from excessively low predicted
329 mixed layer (ML) height (below 200m) at sunset time in three of the days (notice the significant standard
330 deviation of modelled data). This sudden collapse of the ML induces the trapping of pollutants that
331 explains the steep build-up of concentrations at 20h, gradually dispersing within two hours following the
332 decrease in emissions.



333

334 **Figure 8.** Daily average profile of measured (Urb1) and simulated NO_x concentration for the 1 week study period.
335 Vertical bars indicate standard deviation.

336 Table 3 compiles the statistics for the comparison between model outputs and air quality measurements
337 of PM_{10} and NO_x levels considering both hourly and daily averages. Aiming to distinguish the effect of
338 the filtering technique on performance both the direct URBAIR output and with background are shown.
339 As can be seen, model acceptance criteria (cf. section 2.4) are, in general, fulfilled, with a consistent
340 improvement of model accuracy resulting from adding the background contribution, despite some
341 overestimation revealed by the FB, indicating that in some cases the mean bias is not within the
342 threshold of +30% of the mean. In the 24 hours computed record the average r increases significantly
343 from 0.23 to 0.89 by adding the background. Despite the improvement, a poor correlation between
344 observations and predictions is found for the 1h dataset, with an average r of 0.39 (0.08 without the
345 background). This behavior was identified in other studies reporting the application of Gaussian models
346 to line sources emission dispersion (Luhar and Hurley, 2003; Zou et al., 2010; Gibson et al., 2013). The
347 FAC2 parameter, a robust performance measure in the evaluation of Gaussian models, shows that, in
348 average, 78% of the hourly predictions (60% with no background) are within a factor of two of the
349 observations, increasing to 94% (82% without background) for daily averages.

350 **Table 3.** Statistics of URBAIR performance for daily and hourly average concentrations of PM_{10} and NO_x evaluated
351 against observations, without and with (in brackets) the contribution of (filtered) background, for the period
352 between the 1st and the 8th of June. The underlined values indicate that the model acceptance criterion is
353 unfulfilled, while for r (in *italic*) no criterion is available. In the analysis, 174 data points (hourly averages) were
354 considered, except for PM_{10} in Urb1 where the sample was of 91 data points. A positive FB indicates here an over
355 prediction.

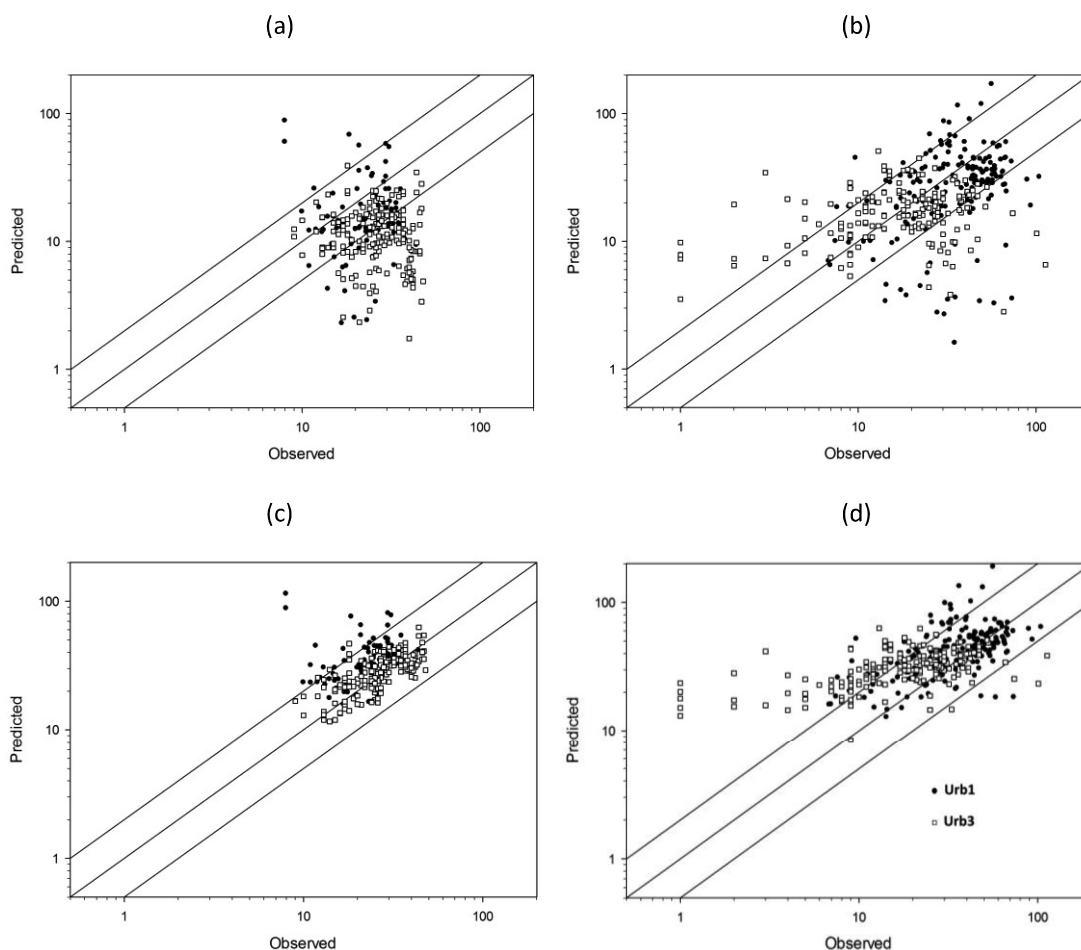
356

	Urb1		Urb3	
	24h	1h	24h	1h
PM10				
NMSE	0.16 (0.15)	0.70 (0.52)	0.91 (0.01)	1.13 (0.08)
FB	-0.33 (0.36)	-0.24 (0.43)	-0.79 (0.03)	-0.78 (0.03)
FAC2	1.00 (1.00)	0.60 (0.79)	0.38 (1.00)	0.42 (0.98)
r	0.51 (0.95)	-0.06 (0.13)	0.11 (0.93)	-0.05 (0.67)
NO_x				
NMSE	0.09 (0.04)	0.55 (0.33)	0.19 (0.17)	0.88 (0.50)
FB	-0.19 (0.17)	-0.18 (0.18)	-0.21 (0.38)	-0.21 (0.37)
FAC2	1.00 (1.00)	0.72 (0.78)	0.88 (0.75)	0.66 (0.55)
r	0.18 (0.79)	0.26 (0.40)	0.11 (0.90)	0.04 (0.37)

357

358 The scatter plot in Figure 9 shows the 1 hour average observed/modelled pairs for different instants in
359 time at each sampling location, the central line indicating a perfect agreement. Figure 9a reinforces the
360 under prediction tendency identified in Table 3 for PM10, while for NO_x a significant dispersion around
361 the 1-to-1 correspondence line is identifiable in Figure 9b, especially at Urb3 spot. The plots (c) and (d)
362 confirm the better agreement between predictions and observations when background is added, despite the overestimation of the lower range of NO_x concentrations at Urb3.

364



365

366

367 **Figure 9.** Scatter plot of observed vs predicted hourly average concentrations (in $\mu\text{g}\cdot\text{m}^{-3}$) of PM10 (a), NO_x (b), PM10
368 with background (c), and NO_x with background (d). Central line indicates a 1-to-1 correspondence, while the upper
369 and bottom lines indicate respectively a factor-of-2 over- and underestimates.

370

371

372 4. Conclusions

373 In this work the air quality of a medium-size European city was simulated, at the urban scale, for a 1
374 week period during which air pollutant concentration measurements were carried out at three distinct
375 spots within the urban area. A modelling approach was applied consisting of (1) detailed traffic flows
376 derived from microscopic traffic models calibrated with GPS data; (2) exhaust road traffic emissions
377 estimated by a combined VSP/EMEP methodology; (3) urban background levels calculated applying a
378 low-pass filter to local air quality observations; and (4) air pollutants dispersion simulated by a second
379 generation Gaussian model accounting for the effects of buildings. The analysis of model performance
380 metrics showed that 78% of the results are within a factor of two of the observations for hourly average
381 concentrations, increasing to 94% when daily averages are considered. The good performance of the
382 model is sustained also by the analysis of the NMSE, which in the great majority of the cases fulfilled the
383 data quality objectives. Despite the low correlation between predicted and observed values for the
384 hourly data series, correlation is shown to significantly improve when urban background concentration
385 is added, with an average of 0.89 for the 24 hours record.

386 In conclusion, the general good agreement obtained between modelling results and local measurements
387 highlights the potential of detailed traffic and instantaneous exhaust emissions data, together with
388 urban background levels extracted from filtered observations, to provide accurate input data to
389 intrinsically simple Gaussian models applied at the urban scale.

390

391 Acknowledgements

392 This work was funded by the Portuguese Science and Technology Foundation (FCT) through projects
393 SMARTDECISION (PTDC/SEN-TRA/115117/ 2009) and PEst-C/ EME/UI0481/2014, the Post-Doctoral
394 scholarship of J.B. Bandeira (SFRH/BPD/100703/2014), and the PhD scholarships of E. Sá
395 (SFRH/BD/60474/2009), P. Fernandes (SFRH/BD/87402/2012) and S. Rafael (SFRH/BD/103184/2014).
396 The authors are grateful for the cooperation of the Institute of Environment and Development (IDAD),
397 Aveiro's city council and Toyota Caetano Portugal during the campaigns.

398

399 References

- 400 ACAP. Automotive Industry Statistics 2010 Edition. ACAP – Automotive Association of Portugal, 2010.
401 Retrieved from <http://www.acap.pt/pt/pagina/36/estat%C3%ADsticas/> in December 2015.
- 402 Ahn K, Rakha H. The effects of route choice decisions on vehicle energy consumption and emissions.
403 *Transp. Res. Part D Transp. Environ.* 2008; 13: 151-167.
- 404 Amirjamshidi G, Mostafa TS, Misra A, Roorda MJ. Integrated model for microsimulating vehicle
405 emissions, pollutant dispersion and population exposure. *Transportation Research Part D: Transport and
406 Environment* 2013; 18: 16–24.
- 407 Amorim JH, Rodrigues V, Tavares R, Valente J, Borrego C. CFD modelling of the aerodynamic effect of
408 trees on urban air pollution dispersion. *Science of the Total Environment* 2013a; 461-462: 541-551.
- 409 Amorim JH, Valente J, Cascão P, Pimentel C, Miranda AI, Borrego C. Pedestrian exposure to air pollution
410 in cities: modelling the effect of roadside trees. *Advances in Meteorology* 2013b; 2013: 964904.

411 Arunachalam S, Valencia A, Akita Y, Serre ML, Omary M, Garcia V, Isakov V. A method for estimating
412 urban background concentrations in support of hybrid air pollution modeling for environmental health
413 studies. *International journal of environmental research and public health* 2014; 11(10): 10518-10536.

414 Bandeira JM, Carvalho D, Asad JK, Roupail NM, Fontes T, Fernandes P, Pereira SR, Coelho MC. Empirical
415 Assessment of Route Choice Impact on Emissions Over Different Road Types, Traffic Demands, and
416 Driving Scenarios. *International Journal of Sustainable Transportation*,
417 <http://dx.doi.org/10.1080/15568318.2014.901447>; in press.

418 Borrego C, Martins JM, Lemos S, Guerreiro C. Second generation Gaussian dispersion model: the
419 POLARIS model. *International Journal of Environment and Pollution* 1997; 8(3/4/5/6): 789–795.

420 Borrego C, Lopes M, Cascao P, Amorim JH, Martins H, Tavares R, Miranda AI, Tallis MJ, Freer-Smith PH.
421 Urban air quality models. In: Chrysoulakis N, Castro E, Moors E, editors. *Understanding urban
422 metabolism: a tool for urban Planning*. UK: Routledge; 2014. p. 79-90.

423 Chang JC, Hanna SR. Air quality model performance evaluation. *Meteorol Atmos Phys* 2004; 87: 167–
424 196.

425 Coelho MC, Frey HC, Roupail NM, Zhai H, Pelkmans L. Assessing methods for comparing emissions from
426 gasoline and diesel light-duty vehicles based on microscale measurements. *Transportation Research
427 Part D* 2009; 14(2): 91–99.

428 Coelho MC, Fontes T, Bandeira J, Pereira S, Tchepel O, Dias D, Sá E, Amorim JH, Borrego C. Assessment
429 of potential improvements on regional air quality modelling related with implementation of a detailed
430 methodology for traffic emissions estimation. *Science of the Total Environment* 2014; 470–471: 127–
431 137.

432 Cyrusa J, Peters A, Soentgen J, Wichmanna H-E. Low emission zones reduce PM10 mass concentrations
433 and diesel soot in German cities. *Journal of the Air & Waste Management Association* 2014; 64(4): 481–
434 487.

435 Denby BR (Ed.). *Guide on modelling Nitrogen Dioxide (NO₂) for air quality assessment and planning
436 relevant to the European Air Quality Directive – Results of activities in the FAIRMODE Working Group 1,
437 Version 4.6, ETC/ACM Technical Paper 2011/15*. Bilthoven, The Netherlands: European Topic Centre on
438 Air Pollution and Climate Change Mitigation (ETC/ACM); 2011. 89 p. Available online at
439 http://acm.eionet.europa.eu/reports/ETCACM_TP_2011_15_FAIRMODE_guide_modelling_NO2.

440 Dowling R, Skabardonis A, Alexiadis V. *Traffic analysis toolbox, volume iii: guidelines for applying traffic
441 microsimulation software – FHWA-HRT-04-040*. Washington DC: FHWA, US Department of
442 Transportation; 2004. 146 pp. Available online at
443 http://ops.fhwa.dot.gov/trafficanalysistools/tat_vol3/vol3_guidelines.pdf.

444 EEA, European Environment Agency. *EMEP/EEA air pollutant emission inventory guidebook 2013 –
445 Technical guidance to prepare national emission inventories*. EEA Technical report No 12/2013.
446 Copenhagen, Denmark: EEA; 2013. 23 pp. doi:10.2800/92722. Available online at
447 <http://www.eea.europa.eu/publications/emep-eea-guidebook-2013>.

448 EEA, European Environment Agency. *The European environment – state and outlook 2015: synthesis
449 report*. Copenhagen, Denmark: EEA; 2015a. 205 pp. doi:10.2800/944899. Available online at
450 <http://www.eea.europa.eu/soer>.

451 EEA, European Environment Agency. Air quality in Europe – 2015 report. EEA Report No 5/2015.
452 Copenhagen, Denmark: EEA; 2015b. 57 pp. doi:10.2800/62459. Available online at
453 <http://www.eea.europa.eu/publications/air-quality-in-europe-2015>.

454 EPA, US Environmental Protection Agency. Methodology for developing modal emission rates for EPA's
455 multi-scale motor vehicle & equipment emission system. Prepared by North Carolina State University for
456 US Environmental Protection Agency, Ann Arbor, 2002. 286 pp. Available online at
457 <http://www3.epa.gov/otaq/models/ngm/r02027.pdf>.

458 EPA, US Environmental Protection Agency. User's guide to the Building Profile Input Program. EPA-
459 454/R-93-038 (October 1993. Revised April 2004). Research Triangle Park, North Carolina 27711, US:
460 EPA, Office of Air Quality Planning and Standards, Technical Support Division; 2004. Available in
461 <http://www3.epa.gov/scram001/userg/relat/bpipdup.pdf>.

462 Fernandes P, Bandeira JM, Fontes T, Pereira SR, Schroeder BJ, Roupail NM, Coelho MC. Traffic
463 restriction policies in an urban avenue: a methodological overview for a trade-off analysis of traffic and
464 emission impacts using microsimulation. *International Journal of Sustainable Transportation* 2016,
465 <http://dx.doi.org/10.1080/15568318.2014.885622>.

466 Fontes T, Fernandes P, Rodrigues H, Bandeira JM, Pereira SR, Khattak A, Coelho MC. Are ecolanes a
467 sustainable option to reduce emissions in a medium-sized european city? *Transport Res A-Pol.* 2014; 63:
468 93–106.

469 Frey HC, Zhang KS, Roupail NM. Fuel use and emissions comparisons for alternative routes, time of day,
470 road grade, and vehicles based on in-use measurements. *Environmental Science & Technology* 2008;
471 42(7): 2483–2489.

472 Gibson MD, Kundu S, Satish M. Dispersion model evaluation of PM_{2.5}, NO_x and SO₂ from point and
473 major line sources in Nova Scotia, Canada using AERMOD Gaussian plume air dispersion model.
474 *Atmospheric Pollution Research* 2013; 4: 157–167.

475 Gidhagen L, Johansson H, Omstedt G. SIMAIR – Evaluation tool for meeting the EU directive on air
476 pollution limits. *Atmospheric Environment* 2009; 43: 1029–1036.

477 Hale D. How many netsim runs are enough?. *McTrans* 1997; 11(3): 1–9.

478 Hyndman R.J., Koehler A.B., Another look at measures of forecast accuracy. *International Journal of*
479 *Forecasting* 2006; 22(4): 679-688.

480 INE, Instituto Nacional de Estatística. Statistical yearbook of Centro Region 2012. Lisbon, Portugal: INE;
481 2013. 512 pp. ISBN 978-989-25-0217-5. Available online at <https://www.ine.pt>.

482 Karamchandani P, Lohman K, Seigneur C. Using a sub-grid scale modeling approach to simulate the
483 transport and fate of toxic air pollutants. *Environmental Fluid Mechanics* 2009; 9: 59–71.

484 Luhar AK, Hurley JP. Evaluation of TAPM, a prognostic meteorological and air pollution model, using
485 urban and rural point-source data. *Atmos. Environ.* 2003; 37: 2795–2810.

486 Mahmood M, Van Arem B, Pueboobpaphan R, Igamberdiev M. Modeling reduced traffic emissions in
487 urban areas: the impact of demand control, banning heavy duty vehicles, speed restriction and adaptive
488 cruise control. 89th Annual Meeting of the Transportation Research Board, Washington DC. 2010. Paper
489 No. 10-3406, 16 pp.

- 490 Martins A, Cerqueira M, Ferreira F, Borrego C, Amorim JH. Lisbon air quality - evaluating traffic hot-
491 spots. *International Journal of Environment and Pollution* 2009; 39(3/4): 306–320.
- 492 Mensink C, Cosemans G. From traffic flow simulations to pollutant concentrations in street canyons and
493 backyards. *Environmental Modelling & Software* 2008; 23(3): 288–295.
- 494 Misra A, Roorda M, MacLean HL. An integrated modelling approach to estimate urban traffic emissions.
495 *Atmospheric Environment* 2013; 73: 81–91.
- 496 PTV, Planung Transport Verkehr. VISSIM users guide. Karlsruhe, Germany: PTV; 2011. 680 pp. Available
497 online at http://www.et.byu.edu/~msaito/CE662MS/Labs/VISSIM_530_e.pdf.
- 498 Schulman LL, Strimaitis DG, Scire JS. Development and evaluation of the PRIME plume rise and building
499 downwash model. *Journal Air Waste Management Association* 2000; 50(3): 378–90.
- 500 Smit R, Brown AL, Chan YC. Do air pollution emissions and fuel consumption models for roadways
501 include the effects of congestion in the roadway traffic flow? *Environmental Modelling & Software*
502 2008; 23: 1262–1270.
- 503 Stein AF, Isakov V, Godowitch J, Draxler RR. A hybrid modeling approach to resolve pollutant
504 concentrations in an urban area. *Atmospheric Environment* 2007; 41(40): 9410–9426.
- 505 Tchepel O, Borrego C. Frequency analysis of air quality time series for traffic related pollutants. *J.*
506 *Environ. Monit.* 2010; 12: 544–550.
- 507 Tchepel O, Costa AM, Martins H, Ferreira J, Monteiro A, Miranda AI, Borrego C. Determination of
508 background concentrations for air quality models using spectral analysis of monitoring data. *Atmos.*
509 *Environ.* 2010; 44: 106–114.
- 510 Tente H, Gomes P, Ferreira F, Amorim JH, Cascão P, Miranda AI, Nogueira L, Sousa S. Evaluating the
511 efficiency of Diesel Particle Filters in high-duty vehicles: field operational testing in Portugal. *Atmos.*
512 *Environ.* 2011; 45: 2623–2629. Valente J, Pimentel C, Tavares R, Ferreira J, Borrego C, Carreiro-Martins P,
513 Caires I, Neuparth N, Lopes M. Individual exposure to air pollutants in a Portuguese urban industrialized
514 area. *J Toxicol Environ Heal Part A* 2014; 77(14–16): 888–899.
- 515 Wesely ML, Doskey PV, Shannon JD. Deposition parameterizations for the Industrial Source Complex
516 (ISC3) model. ANL/ER/TR-01/003. Argonne, Illinois, US: Environmental Research Division, Argonne
517 National Laboratory; 2002.
- 518 Zawar-Reza P, Sturman A, Hurley P. Prognostic urban-scale air pollution modelling in Australia and New
519 Zealand – a review. *Clean Air and environmental Quality* 2005; 39(2): 41–45.
- 520 Zhai H, Frey HC, Roupail NM. Development of a modal emissions model for a hybrid electric vehicle.
521 *Transportation Research Part D* 2011; 16(6): 444–450.
- 522 Zou B, Zhan FB, Wilson JG, Zeng Y. Performance of AERMOD at different time scales. *Simulation*
523 *Modelling Practice and Theory* 2010; 18: 612–623.